



Chinese Materials Research Society

## Progress in Natural Science: Materials International

[www.elsevier.com/locate/pnsmi](http://www.elsevier.com/locate/pnsmi)  
[www.sciencedirect.com](http://www.sciencedirect.com)

## ORIGINAL RESEARCH

# Optimal design of label-free silicon “lab on a chip” biosensors

Yaping Zhang

*Faculty of Engineering, The University of Nottingham Ningbo, Ningbo 315100, China*

Received 7 February 2013; accepted 10 August 2013

Available online 9 October 2013

**KEYWORDS**

Mach-Zehnder  
interferometer;  
Young interferometer;  
Lab on a chip;  
Arrayed biosensors;  
Evanescent field detection

**Abstract** This paper reported the optimal design of label-free silicon on insulator (SOI) “lab on a chip” biosensors. These devices are designed on the basis of the evanescent field detection principles and interferometer technologies. The well-established silicon device process technology can be applied to fabricate and test these biosensor devices. In addition, these devices can be monolithically integrated with CMOS electronics and microfluidics. For these biosensor devices, multi-mode interferometer (MMI) was employed to combine many stand-alone biosensors to form chip-level biosensor arrays, which enable real-time and label-free monitoring and parallel detection of various analytes in multiple test samples. This sensing and detection technology features the highest detection sensitivity, which can detect analytes at extremely low concentrations instantaneously. This research can lead to innovative commercial development of the new generation of high sensitivity biosensors for a wide range of applications in many fields, such as environmental monitoring, food security control, medical and biological applications.

© 2013 Chinese Materials Research Society. Production and hosting by Elsevier B.V. All rights reserved.

## 1. Introduction

It has been more than half a century since the first application of an optical sensing device. There are many optical techniques developed for the detection of various chemical or biochemical interaction, such as surface plasmon resonance (SPR) biosensors, Mach-Zehnder

interferometry biosensors, and Young interferometry biosensors with different degrees of detection sensitivity [1–3]. It comes to light that all the current commercial biosensors have limited usage and detection sensitivity when multiple test samples or target analytes are concerned in the absence of chromophoric or fluorescent labeling substances [3]. Recently, well-established commercial mass production technologies of silicon devices have permitted the pursuing of implementing innovative device concepts in the development of advanced biosensor devices, which would be impossible a few years ago. With the aid of the chip design and micro/nanofabrication technologies, “lab on chip” biosensing devices become a major focus of interdisciplinary research and have attracted significant attentions globally [3–5]. These arrayed biosensing devices incorporate optical wave guide structures with microfluidics at chip level, and therefore exhibit superior functionalities

E-mail address: [yaping.ZHANG@nottingham.edu.cn](mailto:yaping.ZHANG@nottingham.edu.cn)

Peer review under responsibility of Chinese Materials Research Society.



Production and hosting by Elsevier

and capabilities. They are capable of real-time, quantitatively and selectively measuring extremely low concentrations of analyte molecules without using labeling substance [3,4]. In principle, interferometry based integrated opto-fluidic biosensors, such as Mach-Zehnder interferometer [6] and Young interferometer [7], feature the highest detection sensitivity, which are capable of detecting refractive index changes as small as  $10^{-8}$ . Some arrayed interferometry prototype designs at laboratory level for the parallel detection of a number of analytes have been reported [8–10]. However, there is no single commercial device currently available for the detection of multiple analytes in multiple samples at the above highest detection sensitivity.

This work is based on our previous result [3], which makes use of interferometry and evanescent field detection principles and methods. For biosensing device presented in this paper, modular concept is used by employing standard individual stand-alone sensors as modules, which can be combined to form an arrayed biosensing device at chip level. Internal reference channels are integrated on the same sensing chip to compensate for the variations such as the refractive index fluctuations caused by temperature fluctuations, mechanical changes and unknown binding process in the bulk samples, which may affect the accuracy and reliability of detection. Additionally, sensing and reference channels can be grouped at the chip level according to specific requirement. This enables maximal flexibility in measuring individual analytes in multiple test samples simultaneously and instantaneously [3]. For these devices, the detection limit of molecule concentrations at or even below  $10^{-12}$  M can be obtained. The detection sensitivity of the arrayed biosensor here is at least 10–100 times higher than that of the most commonly used commercial SPR biosensors [3].

Optimal simulations and designs were carried out for optimizing of detection sensitivity. The evanescent field penetration depths of the TE and TM fundamental modes were evaluated and compared at the traditional operating wavelength of  $1.55 \mu\text{m}$ . To further increase the evanescent field's penetration depth, a middle infrared wavelength of  $3.39 \mu\text{m}$  was evaluated against  $1.55 \mu\text{m}$  as the operating wavelength.

## 2. Design concept and principles

### 2.1. Parallel detection using arrayed stand-alone interferometry biosensors

Interferometry technologies, such as Mach-Zehnder interferometer (MZI) and Young interferometer (YI), are known to have the

highest detection sensitivity in principle [6–10]. Therefore, the designs presented here use the above interferometers as the stand-alone biosensing modules, which are combined by a multimode interferometers (MMI) optical coupler. Each stand-alone interferometer biosensor module of Mach-Zehnder or Young interferometer can be accessed individually or in a group. Combined with built-in internal reference channels on chip, these biosensor devices allow the maximal flexibility in real-time measuring multiple analytes in multiple test samples. Multiple test solutions are channeled through the arrayed biosensing chip via on-chip microfluidic structures overlaid on top of the optical sensing chip.

Top views of typical optical configurations of proposed “lab on a chip” biosensor devices without microfluidic structures are shown in Fig. 1 [3]. Fig. 1(a) is an arrayed biosensing chip with N stand-alone MZI biosensing modules which were combined with an MMI optical coupler. Fig. 1(b) is an arrayed biosensing chip with N stand-alone YI biosensing modules combined by an MMI optical coupler. For both configurations, by incorporating appropriate microfluidic handling systems, only a single light source is required for the parallel detection of multi-analytes in multi-samples. SU-8 polymer is used in the designs of microfluidic channels overlaid on top of the optical waveguide structures in Fig. 1, to deliver analytes in multiple test samples. For the fabrication of complete opto-fluidic arrayed biosensing chips, the whole optical waveguide chips are covered by SU-8, with channels opened for the delivery of multiple test solutions. These microfluidic structures are then sealed by a top flat plate which was made by polydimethylsiloxane (PDMS) and has fluidic ports for inlet and outlet fluidic connections.

According to the evanescent field detection principle, the biosensing detection of analytes is realized by comparing the phase difference of the propagating light beams through the sensing and reference channels. Phase shift of the sensing channel is caused by a chemical/biochemical/biological reaction over the sensing area, which is quantitatively linked to the concentration of the analytes in the test solution. To be specific, the above phase difference of the sensing and reference channels is related to the effective refractive indices difference of sensing channel ( $N_{\text{eff},s}$ ) and reference channel ( $N_{\text{eff},r}$ ) in stand-alone module biosensing device. It is also related to the interaction length ( $L$ ) of the optical sensing channel, and optical propagation wavelength  $\lambda$ . The phase difference can be expressed by Eq. (1).

$$\phi_{s,r} = \frac{2\pi}{\lambda} [N_{\text{eff},s} - N_{\text{eff},r}]L \quad (1)$$

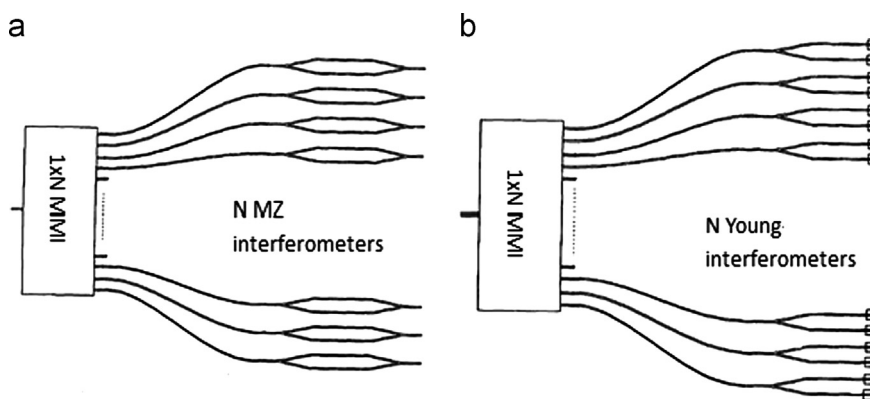


**Fig. 1** Top views of typical arrayed “lab on a chip” biosensing devices: arrayed biosensing chip, with (a) N stand-alone Mach Zehnder interferometers; and (b) N stand-alone Young interferometers, combined by a MMI optical coupler.

## 2.2. Evanescent field detection technology

Opto-fluidic label free “lab on a chip” arrayed biosensors are currently a major interdisciplinary research topic. Research breakthroughs in this area will bring about new generations of biosensing instruments. Evanescent field biosensing devices employing silicon photonic wires have been intensively investigated in the recent years [11–13]. The detection principle of these sensing devices depends mainly on the effective index perturbation of the optical waveguide, which is caused by the interaction of the evanescent field tail of the optical waveguide mode with captured analyte molecules on the sensing surface. As shown in Fig. 2, the propagation light in the photonic wire waveguide extends its guided optical mode as evanescent field into the test solution, which is extremely sensitive to the index change of the surrounding medium. This kind of opto-fluidic evanescent field biosensing devices exhibit very high optical surface sensitivities, allowing the detection of very low analyte concentrations in the test solutions. Interactions of the target analytes in the test solution and the antibody receptor molecules on the sensing surface produce a phase change in the sensing channel and enable the sensitive detection. Normally, the depth of the waveguide evanescent field penetration into the test solution is about a few hundreds of nanometers, as illustrated in Fig. 2.

## 3. Simulations of a label-free arrayed opto-fluidic biosensing device

### 3.1. Simulation structure

The simulation model is shown in Fig. 3 with a side view of the device shown in Fig. 3(a). The simulation model for the cross-section equivalent is shown in Fig. 3(b).

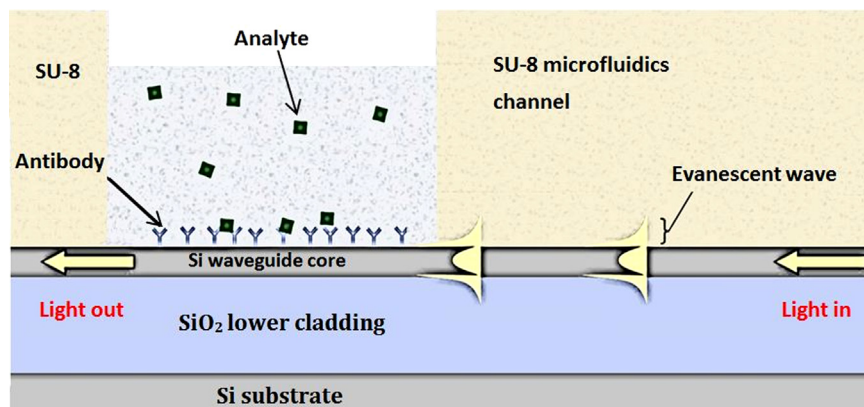


**Fig. 2** Side view of a sensing channel in an evanescent field biosensor, which illustrates the principle of evanescent field detection for an opto-fluidic biosensor.

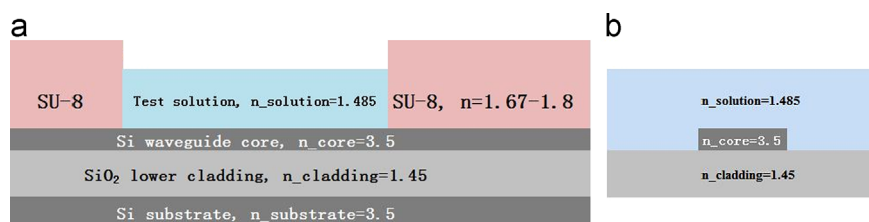


**Fig. 3** (a) Illustrations of the configuration of the SOI material system for the biosensor; and (b) shows the cross-section equivalent simulation model of a silicon photonic wire covered by test solution, on top of the SiO<sub>2</sub> lower cladding layer.

The sensing channels are functionalized by antibody receptor molecules to capture specific target analytes. As the refractive index for majority test solutions is in the range of 1.464–1.476 and 1.495–1.510, a covering refractive index of 1.485 is therefore to be chosen in the simulation model, as shown in Fig. 3(b). Evanescent field penetration depth into the test solution is used as an indication to maximize the detection sensitivity. Detailed optimal simulations and designs are presented below.

### 3.2. Comparative study for the TE and TM evanescent field penetration

Simulations were carried out for the calculations of evanescent field penetrations for both transverse electric mode (TE) and transverse magnetic mode (TM) polarizations at the operating wavelength of 1.55  $\mu\text{m}$ . The silicon wire width is chosen as 2  $\mu\text{m}$  and its thickness is varied from 0.22  $\mu\text{m}$  to 0.5  $\mu\text{m}$ .

Fundamental TE and TM modes with their vertical optical fields and the refractive index profiles of a structure of silicon core thickness of 0.34  $\mu\text{m}$  are shown in Fig. 4. SOI wafer with this silicon core thickness is commercially available.

From Fig. 4(a)–(d), it can be seen that the amount of TM mode's evanescent field is much bigger than that of TE mode. The penetration depth of the TM mode is deeper than that of the TE mode. This has been further illustrated in the simulation results in Fig. 5 with the calculations of the evanescent field penetrations for varied silicon wire thickness for both TE and TM modes.

### 3.3. Extend the evanescent field penetration depth with longer operating wavelength

SOI has been used as the platform for near infrared operating wavelength of 1.55  $\mu\text{m}$  due to its lower optical propagation loss at

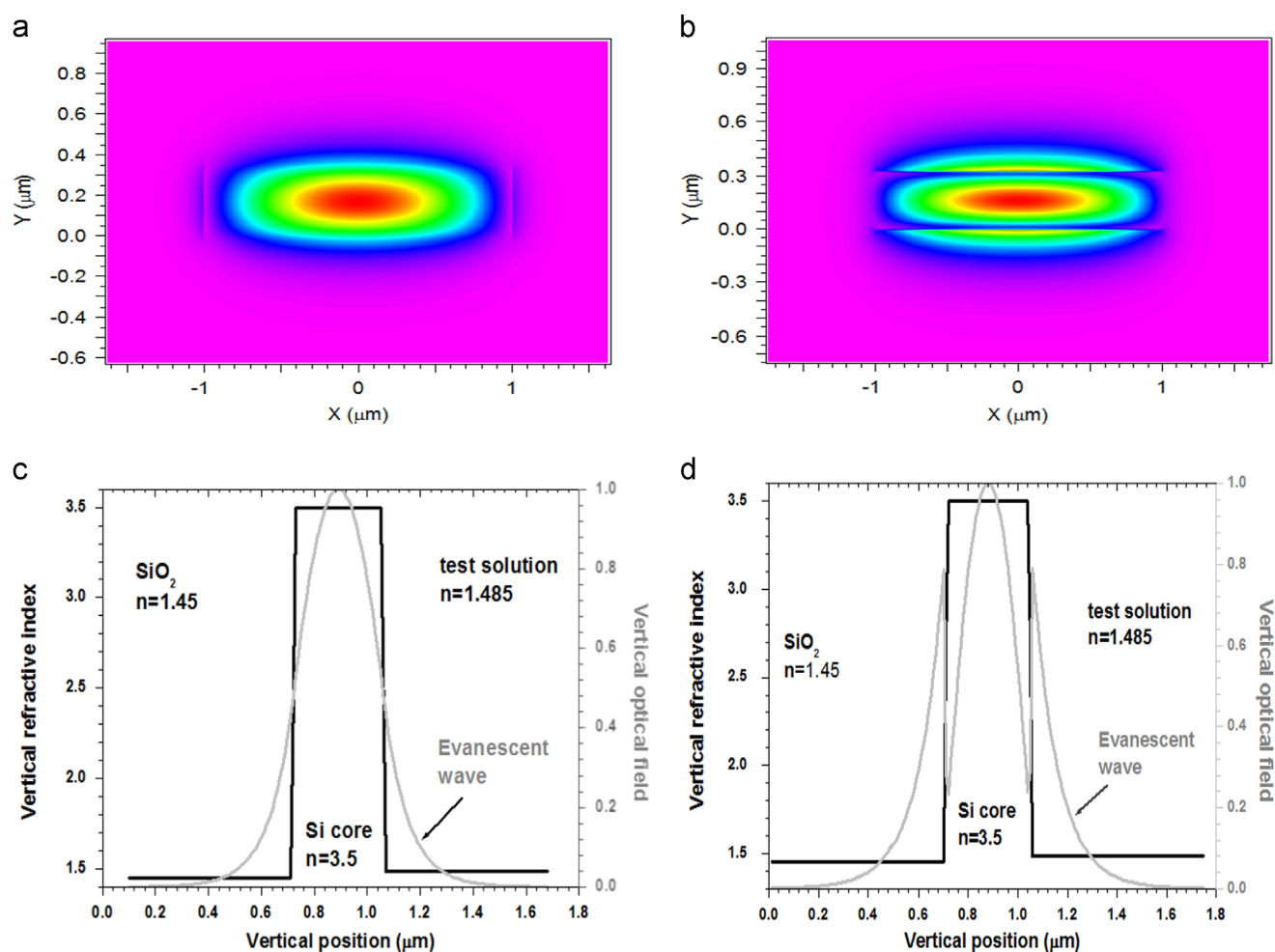


Fig. 4 Fundamental TE (a) and TM (b) modes, and the vertical optical fields and refractive index profiles of TE (c) and TM (d).

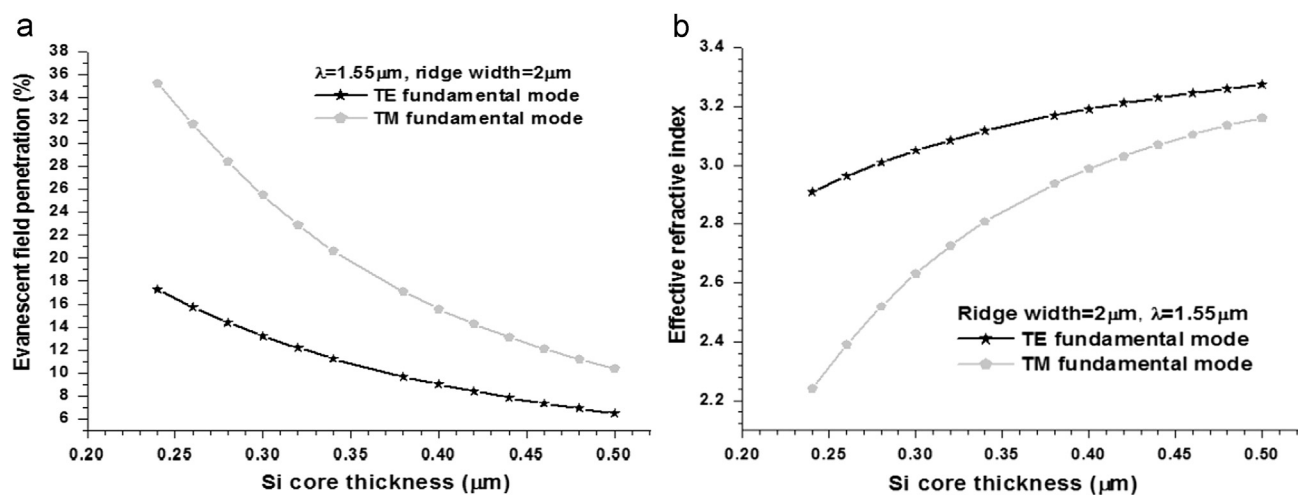
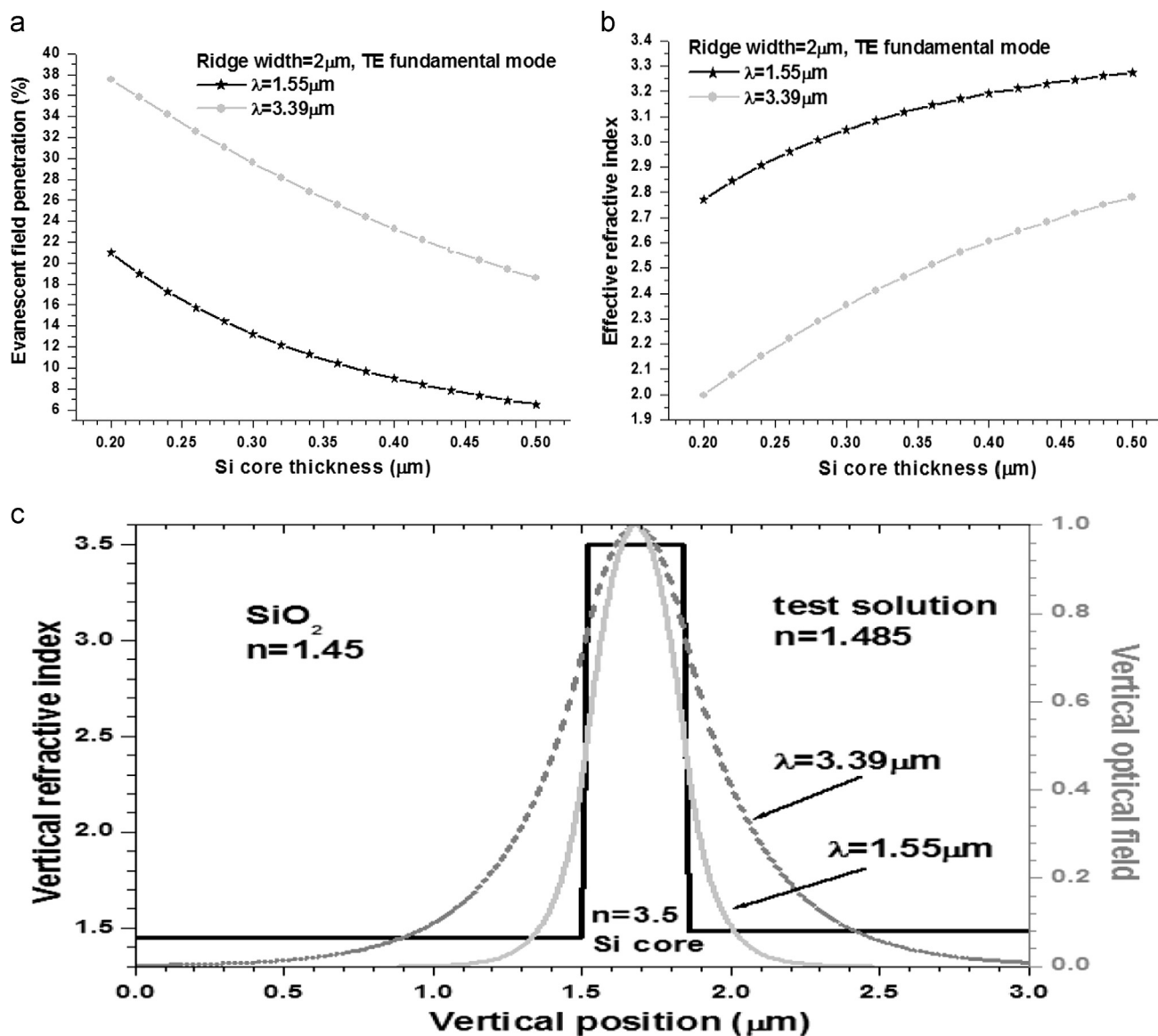


Fig. 5 Evanescent field penetration simulation results for varied silicon wire thickness for the TE and TM fundamental mode. (a) Evanescent field penetration percentages for TE and TM fundamental modes. (b) Effective refractive indices for TE and TM fundamental modes.

this operating wavelength. However, recent research shows that comparatively lower propagation loss of 0.6–0.7 dB/cm can be achieved at the operating wavelength of 3.39  $\mu\text{m}$  [14]. This extends the SOI applications to the middle infrared region where biomedical or biosensing applications are of greater importance.

Simulations were carried out for the above structure in Fig. 3(b) at an operating wavelength of 3.39  $\mu\text{m}$ . The results were compared with those obtained at the wavelength of 1.55  $\mu\text{m}$  and shown in Fig. 6. Fig. 6 shows the evanescent field penetration depth at the wavelength of 3.39  $\mu\text{m}$  is much bigger than that at the wavelength



**Fig. 6** Comparison of vertical evanescent field penetration depths at the operating wavelengths of 1.55  $\mu\text{m}$  and 3.39  $\mu\text{m}$ . (a) Evanescent field penetration percentages at the wavelengths of 1.55  $\mu\text{m}$  and 3.39  $\mu\text{m}$  for varied silicon wire thickness and fixed ridge width of 2  $\mu\text{m}$ ; (b) Effective refractive indices corresponding to the above case. (c) Vertical optical field profiles for the fundamental mode at the wavelengths of 1.55  $\mu\text{m}$  and 3.39  $\mu\text{m}$  for a given structure of silicon wire thickness of 0.34  $\mu\text{m}$ .

of 1.55  $\mu\text{m}$ . This indicates that the evanescent field penetration depth can be increased by using longer operating wavelength.

With regard to alternative middle infrared materials, chalcogenide glasses have been proven to be suitable for biosensing applications [15], and can be mass-produced by hot-embossing methods [16,17].

#### 4. Discussion and conclusions

The design concept and principle of arrayed “lab on a chip” opto-fluidic biosensing devices are introduced. Optimal simulations and designs were presented in terms of optimizing the detection sensitivity via maximizing the evanescent field penetration depth into the test solution. Simulation results show that transverse magnetic (TM) polarization optical field has deeper penetration depth compared with that of the TE. Simulation results also show

that evanescent field penetration depth can be further extended by using middle infrared wavelength. The complete structure of the arrayed “lab on a chip” devices can be designed based on the optimized epilayer structure simulation results, which were presented, complemented by further simulations and designs of bend waveguide with minimal loss and optimized MMI optical coupler. Various functionalities of them can be realized by in cooperation with various microfluidics configurations. This research will enable the explorations of next generation of low-cost opto-fluidic biosensors and trigger the modern analytical technology revolutions.

#### Acknowledgments

The author gratefully acknowledges the financial support of the University of Nottingham Ningbo China.



## References

- [1] A. Abbas, M.J. Linman, Q. Cheng, *Biosensors and Bioelectronics* 26 (2011) 1815–1824.
- [2] F. Prieto, B. Sepulveda, A. Calle, A. Llobera, C. Dominguez, A. Abad, A. Montoya, L.M. Lechuga, *Nanotechnology* 14 (2003) 907–912.
- [3] Y. Zhang, GB2437543, 2010.
- [4] X. Fan, I.M. White, *Nature Photonics* 5 (2011) 591–597.
- [5] A.L. Washburn, R.C. Bailey, *Analyst* 136 (2010) 227–236.
- [6] R.G. Heideman, P.V. Lambeck, *Sensors and Actuators B* 61 (1999) 100–127.
- [7] A. Brandenburg, *Sensors and Actuators B* 38–39 (1997) 266–271.
- [8] R. Bernini, A. Cusano, *Sensors and Actuators B* 100 (2004) 72–74.
- [9] A. Ymeti, J.S. Kanger, R. Wijn, P.V. Lambeck, R.J. Greve, *Sensors and Actuators B* 83 (2002) 1–7.
- [10] A. Ymeti, J.S. Kanger, J. Greve, G.A.J. Besselink, P.V. Lambeck, R. Wijn, R.G. Heideman, *Biosensors and Bioelectronics* 20 (2005) 1417–1421.
- [11] A. Cleary, S. García-Blanco, A. Glidle, et al., *IEEE Sensors Journal* 5 (2005) 1315–1320.
- [12] A. Densmore, D.-X. Xu, P. Waldron, S. Janz, P. Cheben, J. Lapointe, A. Delage, *IEEE Photonics Technology Letters* 18 (2006) 2520–2522.
- [13] A. Densmore, M. Vachon, D.-X. Xu, S. Janz, R. Ma, Y.-H. Li, G. Lopinski, A. Delage, J. Lapointe, C.C. Luebbert, Q.Y. Liu, P. Cheben, J.H. Schmid, *Optics Letters* 34 (2009) 3598–3600.
- [14] G.Z. Mashanovich, M.M. Milosevic, M. Nedeljkovic, N. Owens, B. Xiong, E.J. Teo, Y. Hu, *Optics Express* 19 (2011) 7112–7119.
- [15] J. Hu, N. Carlie, N.-N. Feng, L. Petit, A. Agarwal, K. Richardson, L. Kimerling, *Optics Letters* 33 (2008) 2500–2502.
- [16] W.J. Pan, H. Row, D. Zhang, Y. Zhang, et al., *Microwave and Optical Technology Letters* 50 (2008) 1961–1963.
- [17] A.B. Seddon, W.J. Pan, D. Furniss, A. Miller, A. Row, D. Zhang, Y. Zhang, et al., *Journal of Non-Crystalline Solids* 352 (2006) 2515–2520.